

Positive exchange biasing in GdFe/NiCoO bilayers with antiferromagnetic coupling

D. Z. Yang,^{1,4} J. Du,^{2,3} L. Sun,³ X. S. Wu,³ X. X. Zhang,² and S. M. Zhou^{1,3,*}

¹*Surface Physics Laboratory (National Key Laboratory) and Department of Physics, Fudan University, Shanghai 200433, People's Republic of China*

²*Department of Physics, Hong Kong University of Science & Technology, Kowloon, Hong Kong, People's Republic of China*

³*State Key Laboratory of Solid State Microstructures, Nanjing University, Nanjing 210093, People's Republic of China*

⁴*Department of Physics, Southeast University, Nanjing 210096, People's Republic of China*

(Received 27 October 2004; revised manuscript received 21 December 2004; published 25 April 2005)

For GdFe/NiCoO bilayers after field cooling, hysteresis loops at low temperatures are shifted along both the horizontal and vertical axes. The exchange field H_E changes from negative values to positive values with increasing cooling field H_{CF} and the coercivity H_C acquires a maximum near the crossover of H_E . At 5 K, H_E and H_C at $H_{CF}=3$ T and the peak height ΔH_C are proportional to the inverse GdFe layer thickness. At $H_{CF}=3$ T, H_E is always positive in the temperature region from 5 to 350 K. At low H_{CF} , however, H_E is negative at low temperatures and becomes positive at high temperatures. These results can be ascribed to antiferromagnetic coupling between GdFe and NiCoO layers.

DOI: 10.1103/PhysRevB.71.144417

PACS number(s): 75.30.Gw, 75.30.Et, 75.70.Cn

Positive exchange biasing (EB) has first been observed in a variety of antiferromagnet (AF)/ferromagnet (FM) bilayers with AF materials fluorides, in which the FM and AF layers were argued to have antiferromagnetic coupling at the interface.¹ It has been detected recently in ferrimagnet/ferrimagnet, FM/ferrimagnet bilayers with antiferromagnetic coupling and other systems.²⁻⁷ These bilayers have two additional distinguished features. First, the exchange field H_E has a crossover from negative values to positive values at a critical value of the cooling field H_{CF}^0 . Second, the coercivity H_C has a maximum at H_{CF}^0 , in addition to the normal enhancement due to the EB.⁸ Apparently, the EB strongly depends on the magnitude of the cooling field H_{CF} . It is quite different from conventional FM/AF bilayers with ferromagnetic coupling, in which H_E and H_C are almost independent of H_{CF} if it is larger than the saturation field of the FM layer.^{9,10} In the strict sense, the positive EB has been found only in a few FM/AF systems.²⁻⁷ Therefore, extensive studies on the mechanism of the positive EB have been hindered and more experiments are required.

In this paper, we will study the EB phenomena in FM/AF bilayers by using GdFe(=Gd₄₅Fe₅₅)/NiCoO(=Ni₄₆Co₅₄O) bilayers, where NiCoO and GdFe are typical AF material and ferrimagnetic alloys, respectively.^{2,11} The atomic magnetic moment of Gd comes from spin and orbital angular momentums and both of them are parallel to the atomic magnetic moment. The atomic magnetic moment of Fe is contributed only from the spin angular momentum because the orbital angular momentum is almost quenched. Due to antiferromagnetic coupling between the spins of Gd and Fe, the atomic magnetic moment of Gd is aligned antiparallel to that of Fe and the macroscopic magnetization of Gd₄₅Fe₅₅ alloys is parallel to that of Gd atoms since the latter is dominant. More remarkably, the magnetizations of NiCoO and GdFe layers can have antiferromagnetic coupling at the interface when the contribution of Gd atoms is larger than that of Fe atoms. This is because the atomic magnetic moment of Gd should also be coupled to Co and Ni atoms in AF bilayers

antiferromagnetically at the interface. The compositions of the NiCoO and GdFe layers are selected so that the Néel temperature of the AF layer is lower than the Curie temperature of the GdFe layer and FM and AF layers are coupled *antiferromagnetically*, where the Néel temperature of the NiCoO layer is 400 K and the Curie temperature of the GdFe layer is 430 K.¹¹⁻¹³

A large specimen of GdFe/NiCoO (20 nm) bilayer was deposited on Si(100) at ambient temperature by magnetron sputtering system. The base pressure was 2×10^{-5} Pa and the Ar pressure 0.33 Pa during deposition. GdFe and NiCoO layers were made from GdFe and NiCoO composite targets by dc and rf sputtering, respectively. In experiments, small Gd pieces were put on Fe target and small pieces of CoO on NiO target to form GdFe and NiCoO composite targets. The growth rates of GdFe and NiCoO layers were 0.1 and 0.04 nm/s, respectively. The FM layer has a wedge shape to alleviate the run-to-run variation. During deposition, a magnetic field of about 130 Oe was applied parallel to the film plane and along the wedge direction to induce an in-plane uniaxial anisotropy in the FM layer. To analyze the magnetic properties, in-plane hysteresis loops were measured by superconductivity quantum interference device. Before measurements, a large specimen was cut into small pieces along the wedge direction. Each sample was heated to 370 K and cooled to 5 K under an external magnetic field and hysteresis loops were then measured during warming up. During field cooling and measurements, the external magnetic field is aligned along the wedge direction. The compositions of NiCoO and GdFe layers were analyzed by x-ray fluorescence. Structural characterization was carried out by x-ray diffraction. GdFe layers are amorphous and NiCoO layers polycrystalline with preferred (002) orientation.

Figure 1 shows typical hysteresis loops of GdFe(15 nm)/NiCoO(20 nm) bilayers at 5 K, where $H_{CF}=3$ T, 0.5 T, and 150 Oe. One can find that hysteresis loops are shifted away from the zero magnetic field. H_E is positive for $H_{CF}=3$ T and negative for $H_{CF}=150$ Oe. Moreover, H_C

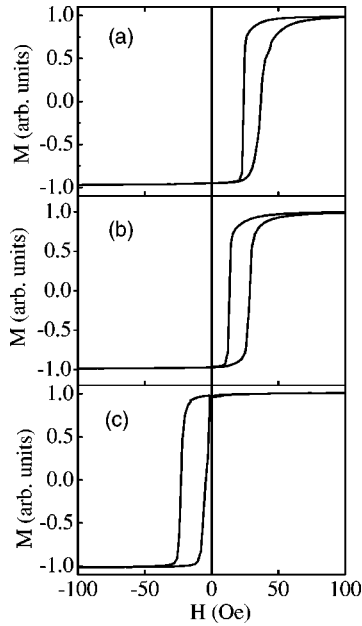


FIG. 1. Typical in-plane hysteresis loops of GdFe(15 nm)/NiCoO(20 nm) bilayers at 5 K, with H_{CF} of 3 T (a), 0.5 T (b), and 150 Oe (c).

for $H_{CF} = 150$ Oe is larger than that of $H_{CF} = 3$ T. Remarkably, the hysteresis loop has a prominent asymmetry for $H_{CF} = 3$ T and the asymmetry becomes weak as H_{CF} is decreased. Figure 2(a) shows the variation of H_E at 5 K as a function of H_{CF} for GdFe/NiCoO bilayers with different FM thickness t_{FM} . With increasing H_{CF} , H_E for all samples changes sharply from negative to positive at small H_{CF} and finally approaches to saturate. The critical value H_{CF}^0 for the crossover does not significantly with t_{FM} . Figure 2(b) shows that for all t_{FM} , H_C increases sharply with initially increasing H_{CF} and reaches a maximum. Finally, it decreases to reach a constant as H_{CF} is further increased. Fortunately, the maxi-

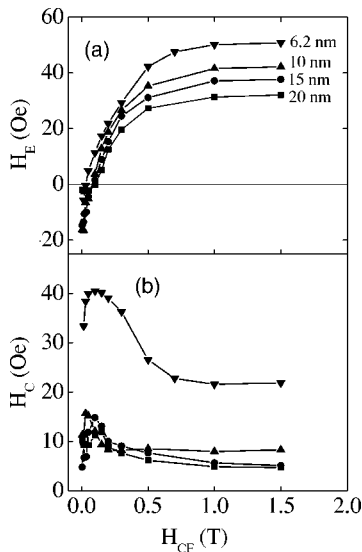


FIG. 2. Dependence of H_E (a) and H_C (b) at 5 K on H_{CF} for GdFe/NiCoO (20 nm) bilayers with a variety of t_{FM} , as denoted by the inset numbers.

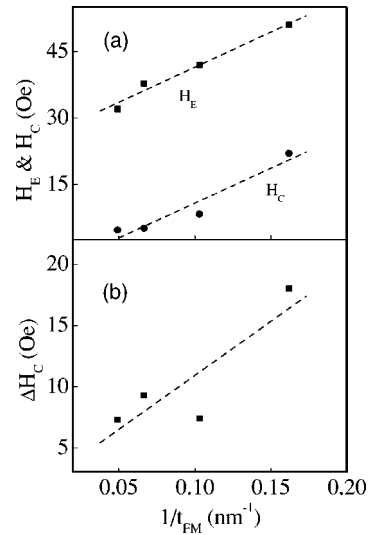


FIG. 3. The t_{FM} dependence of H_E and H_C (a) and the additional coercivity enhancement ΔH_C (b) for GdFe/NiCoO (20 nm) bilayers, where H_{CF} is 3 T and temperature is 5 K.

imum H_C is located near H_{CF}^0 . At $H_{CF} = 3$ T, H_E and H_C increase with decreasing t_{FM} as a result of the interfacial nature of the exchange biasing in the GdFe/NiCoO bilayers.

Figure 3 shows H_E and H_C at 5 K and $H_{CF} = 3$ T for GdFe/NiCoO (20 nm) bilayers as a function of t_{FM} . H_E is approximately proportional to $1/t_{FM}$, demonstrating an interfacial nature of the EB, as shown in Fig. 3(a). According to the slope of the curve H_E vs $1/t_{FM}$, the exchange coupling energy can be calculated. For GdFe/NiCoO bilayers, it is 0.06 erg/cm². Since H_C of corresponding free single layer films is as small as few oersteds (not shown), the enhanced H_C of bilayers is proportional to $1/t_{FM}$, as shown in Fig. 3(a). From Fig. 3(a), one can know that the right coercivity of the hysteresis loop $H_{C1} (= H_E + H_C)$ changes sharply with t_{FM} while the left coercivity $H_{C2} (= H_E - H_C)$ is almost independent of t_{FM} . In this way, one can know that for the ascent branch of the wedged FM layers the magnetization reversal process is accompanied by a motion of a single domain wall while for the descent branch it is accompanied by the nucleation of the multidomains and motion of the domain walls. The right and left branches of the loop are thought to have different magnetization reversal process.^{14,15} In Fig. 2, we define the $\Delta H_C = H_C^{\max} - H_C^{\min}$, where H_C^{\max} and H_C^{\min} are the coercivity of the sample near H_{CF}^0 and at $H_{CF} = 3$ T, respectively. At 5 K, ΔH_C is found to decrease as t_{FM} is increased and the dependence can be approximately fitted by the scale of $\Delta H_C \propto 1/t_{FM}$, as shown in Fig. 3(b).

Figure 4 shows the temperature dependence of H_E and H_C for GdFe(15 nm)/NiCoO(20 nm) bilayer with two different H_{CF} . For $H_{CF} = 3$ T, H_E is always positive at all temperatures, as shown in Fig. 4(a). It decreases monotonically with increasing temperature and approaches zero near 350 K. H_C changes with temperature in a similar way. Apparently, the large H_C is caused by the establishment of the EB. It is of particular interest to find different temperature dependence for small H_{CF} . As shown in Fig. 4(b), at low temperatures, H_E is negative and becomes positive at temperatures above

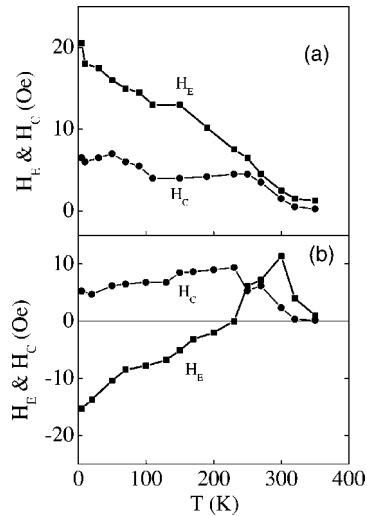


FIG. 4. Temperature dependence of H_E and H_C at $H_{CF}=3$ T (a) and 150 Oe (b) for GdFe(15 nm)/NiCoO(20 nm) bilayers.

250 K. H_C increases slightly with rising temperature and acquires a maximum near 250 K, i.e., the same temperature for the crossover of H_E .

We have carefully compared the hysteresis loops of GdFe(6.2 nm)/NiCoO(20 nm) bilayers at different H_{CF} in Fig. 5. One can find that when H_{CF} is 50 Oe and 15 kOe, the exchange field is -14 and 39 Oe, respectively. More remarkably, the inset shows $m_t(+H)(15 \text{ kOe}) > m_t(+H)(50 \text{ Oe})$. Actually, at negative saturation field $|m_t(-H)(15 \text{ kOe})| < |m_t(-H)(50 \text{ Oe})|$, that is to say, the hysteresis loop with positive EB is shifted towards positive magnetization axis, in comparison with negative EB. For $H_{CF}=15$ kOe, the positive shift amount Δm is about 3×10^{-6} emu for a sampling area of 0.25 cm^2 , which is equivalent to the magnetic moment of 1 ML FM or AF layers.

All the above results for GdFe/NiCoO bilayers are similar to the observed phenomena in fluoride based bilayers and

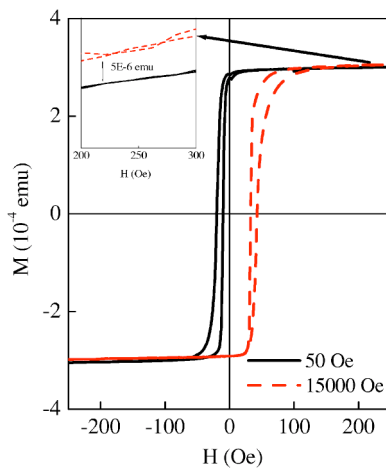


FIG. 5. (Color online) Typical hysteresis loops at 5 K for GdFe(6.2 nm)/NiCoO(20 nm) bilayers with cooling fields of 15 kOe and 50 Oe. The inset enlarges the curve of magnetization vs magnetic field in the saturation region. The inset numbers refer to the cooling fields.

those of GdFe/TbFe bilayers.^{1,2,8,16,17} Below we will analyze the above experimental results and reveal the mechanism behind them. Few models were proposed to explain the positive EB in Fe/FeF₂ and Fe/MnF₂ bilayers.^{18–21} The evolution of H_E and H_C with H_{CF} was thought to originate from the competition between the Zeeman energy of the AF spins in an external magnetic field and antiferromagnetic coupling. In Gd–Fe/Tb–Fe bilayers with antiferromagnetic coupling, however, the positive H_E was explained in terms of the hybrid domain wall near interface.²

It is instructive to first analyze the vertical magnetization shift at different H_{CF} for GdFe/NiCoO bilayers. In general, the hysteresis loops of free FM layer films should be centered about the horizontal axis. For the present GdFe/NiCoO bilayers, however, the hysteresis loop is shifted along the vertical axis because of two possible reasons. First, a domain wall might be formed in the GdFe layer parallel to the film plane, which was argued to exist in ferrimagnet/ferrimagnet bilayers.² For positive EB, the domain wall will be formed at large positive magnetic field and thus the magnitude of the magnetization at positive saturation magnetic field is reduced, that is to say, $|m_{FM}(+H)| < |m_{FM}(-H)| = m_{FM}(\text{saturation})$ and vice versa for negative EB, $|m_{FM}(-H)| < |m_{FM}(+H)| = m_{FM}(\text{saturation})$. Therefore, the vertical shift Δm_{FM} is negative and positive for positive and negative EB, respectively. Second, an additional small magnetic moment Δm_{AF} might be contributed from the AF layers, which cannot be altered within the measuring magnetic field.¹⁷ For positive and negative EB, Δm_{AF} has positive and negative signs and thus the hysteresis loop should be shifted towards positive and negative magnetization axis, respectively. The total vertical shift of the hysteresis loops consists of two parts and $\Delta m = \Delta m_{AF} + \Delta m_{FM}$.

At least, one can draw two conclusions from the results in Fig. 5. First, Δm_{AF} is not equal to zero. Otherwise, $m_t(+H)(15 \text{ kOe}) \leq m_t(+H)(50 \text{ Oe})$ with FM domain wall or without any FM domain wall. The results in the inset are in agreement with the fact that Δm_{AF} is positive for $H_{CF} = 15$ kOe and negative for $H_{CF} = 50$ Oe. Second, no domain wall parallel to the film plane exists in the FM layers. This is because Δm is about the magnetic moment of 1 ML AF layer and equivalent to Δm_{AF} . Therefore, Δm_{FM} must be equal to zero and thus no FM domain wall parallel to the film plane exists in the GdFe layer. In a word, the so-called hybrid domain wall model can be excluded in the explanations of the present results.²

The evolution of the exchange field with H_{CF} in Fig. 2 can be explained as a result of the competition between antiferromagnetic coupling energy of FM and AF spins and the Zeeman energy of the AF spins with the external magnetic field H_{CF} . For a large/small H_{CF} , the AF spins are aligned parallel/antiparallel to H_{CF} and the FM spins. After field cooling procedure, the AF spins at low temperatures are of a meta-stable/stable state, i.e., in high/low energy state. Therefore, the positive/negative H_E can be induced and there should be a critical value H_{CF}^0 for the crossover of H_E . It can be estimated as follows:¹

$$H_{\text{CF}}^0 = - \frac{(J_1 S_{\text{AF}} S_{\text{Fe}} + J_2 S_{\text{AF}} S_{\text{Gd}})}{M_{\text{AF}}}, \quad (1)$$

where S_{Fe} is the spins of Fe atoms near interface, S_{Gd} the spins of Gd atoms, and S_{AF} the AF spins. J_1 and J_2 are the exchange interaction constants of Fe and Gd spins with AF spins, respectively. M_{AF} is the net magnetization of the AF material, which was observed before in fluoride based FM/AF bilayers.¹⁷ Apparently, above equation shows that H_{CF}^0 is independent of the FM and AF layer thickness, as observed in Fig. 2. Since J_1 and J_2 have opposite signs, H_{CF}^0 in the GdFe/NiCoO and GdFe/TbFe bilayers is much smaller than those of Fe/FeF₂ and Fe/MnF₂ bilayers.^{1,2}

Since a multi-domain structure in the AF layer is formed and then fixed after field cooling procedure, an additional pinning effect of the AF domain walls on the motion of the FM domain wall exists,^{8,22} and ΔH_C can be expressed in terms of the domain size in FM and AF bilayers as follows:

$$\Delta H_C = \frac{J_{\text{eff}}}{t_{\text{FM}} M_{\text{FM}} d_{\text{AF}} a_0^2} L_{\text{FM}}, \quad (2)$$

where J_{eff} is the effective interaction between FM and AF layers and a_0 is the interfacial atomic separation in the FM layer. L_{FM} is the length of the FM domain wall under consideration and d_{AF} the domain size of the AF layer. Since the number of the AF domain has a maximum and thus d_{AF} has a minimum at H_{CF}^0 , the ΔH_C has a maximum near the crossover. As the FM layer has a wedged shape, the motion of a single domain wall occurs during magnetization reversal process, which is perpendicular to the wedge direction. Therefore, L_{FM} , taking the sample size perpendicular to the wedge direction (about 3 mm), is independent of t_{FM} ,²³ ΔH_C should be inverse proportional to t_{FM} . In a word, one can find that Eq. (2) can be used to explain the results in Figs. 2(b) and 3(b).

The evolution of H_E with temperature at different H_{CF} in Fig. 4 can be explained as follows. First, in FM/AF bilayers with antiferromagnetic coupling, the change in the sign of H_E comes from the competition of the Zeeman energy of the AF spins in the external magnetic field and the antiferromagnetic coupling between the FM and AF layers.²¹ Second, at low temperatures the exchange biasing can be produced not only by the effect of the field cooling through the Néel temperature of the AF layers, but also by the accumulation effect

of field cooling from temperatures lower than the Néel temperature to the sampling temperature.²⁴ This is a so-called memory effect. In the present work, the exchange biasing was established by a field cooling procedure from 370 K, which is lower than the the Néel temperature of the AF layer. At very small H_{CF} , the Zeeman energy cannot overcome the antiferromagnetic coupling at any temperature in the region presented here, and thus the AF and FM spins are aligned antiparallel to each other. H_E is negative at all temperatures. Similarly, one can understand the reason that H_E is always positive at the whole measuring temperature region for high H_{CF} . At an intermediate H_{CF} , the coupling energy is larger than the Zeeman energy at low temperatures and the former one is smaller than the latter at high temperatures since the interfacial exchange coupling energy weakens at high temperatures. Therefore, H_E is negative and positive at low and high temperatures, respectively.

In summary, we have prepared GdFe/NiCoO (20 nm) bilayers with a wedged FM layer and studied the EB as a function of H_{CF} , temperature, and the GdFe layer thickness. As H_{CF} is increased, H_E changes from negative values to positive values with a crossover at H_{CF}^0 and finally approaches saturation, and H_C acquires an additional enhancement near H_{CF}^0 . H_E and H_C for $H_{\text{CF}}=3$ T, and ΔH_C are proportional to the inverse GdFe layer thickness. At $H_{\text{CF}}=3$ T, H_E is positive in the entire temperature region. At low H_{CF} , however, H_E is negative at low temperatures and becomes positive at high temperatures. For GdFe/NiCoO bilayers, the magnetization shift is positive and negative for positive and negative EB, respectively. It is proposed that there is no FM domain wall parallel to the film plane during FM magnetization reversal process. The present results can be attributed to a competition between the antiferromagnetic coupling at the GdFe/NiCoO interface and the Zeeman energy of the AF spins in the H_{CF} .

This work was supported by the National Natural Science Foundation of China Grant Nos. 10174014, 60271013, 10021001, 10321003, 60490290, and 10474038, and the State Key Project of Fundamental Research Grant Nos. 2001CB610602 and 2002CB613504, and Shanghai Nanotechnology Program Center (No. 0252nm004). J.D. and X.X.Z. thank the support of Hong Kong RGC (HKUST6165/01P)

*Electronic address: shimingzhou@yahoo.com

¹J. Nogués, D. Lederman, T. J. Moran, and I. K. Schuller, Phys. Rev. Lett. **76**, 4624 (1996).

²S. Mangin, F. Montaigne, and A. Schuhl, Phys. Rev. B **68**, 140404 (2003).

³F. Canet, C. Bellouard, S. Mangin, C. Chatelain, C. Senet, R. Siebrecht, V. Leiner, and M. Picuch, Eur. Phys. J. B **34**, 381 (2003).

⁴T. L. Kirk, O. Hellwig, and E. E. Fullerton, Phys. Rev. B **65**, 224426 (2002).

⁵R. L. Compton, M. J. Pechan, S. Maat, and E. E. Fullerton, Phys. Rev. B **66**, 054411 (2002).

⁶C. Prados, E. Pina, A. Hernando, and A. Montone, J. Phys.: Condens. Matter **14**, 10063 (2002).

⁷T. Gredig, I. N. Krivorotov, P. Eames, and E. D. Dahlberg, Appl. Phys. Lett. **81**, 1270 (2002).

⁸C. Leighton, J. Nogués, B. J. Jönsson-Åkerman, and I. K. Schuller, Phys. Rev. Lett. **84**, 3466 (2000).

⁹T. J. Moran and I. K. Schuller, J. Appl. Phys. **79**, 5109 (1996).

¹⁰T. Ambrose and C. L. Chien, J. Appl. Phys. **83**, 7222 (1998).

- ¹¹T. Ambrose, K. Liu, and C. L. Chien, *J. Appl. Phys.* **85**, 6124 (1999).
- ¹²A. J. Devasahayam and M. H. Kryder, *IEEE Trans. Magn.* **35**, 649 (1999).
- ¹³N. Nishimura, T. Hiroki, T. Okada, and S. Tsunashima, *J. Appl. Phys.* **79**, 5863 (1996).
- ¹⁴V. I. Nikitenko, V. S. Gornakov, L. M. Dedukh, Y. P. Kabanov, A. F. Khapikov, A. J. Shapiro, R. D. Shull, A. Chaiken, and R. P. Michel, *Phys. Rev. B* **57**, R8111 (1998).
- ¹⁵M. R. Fitzsimmons, P. Yashar, C. Leighton, I. K. Schuller, J. Nogués, C. F. Majkrzak, and J. A. Dura, *Phys. Rev. Lett.* **84**, 3986 (2000).
- ¹⁶H. T. Shi, D. Lederman, N. R. Dilley, R. C. Black, J. Diedrichs, K. Jensen, and M. B. Simmonds, *J. Appl. Phys.* **93**, 8600 (2003).
- ¹⁷J. Nogués, C. Leighton, and Ivan K. Schuller, *Phys. Rev. B* **61**, 1315 (2000).
- ¹⁸T. M. Hong, *Phys. Rev. B* **58**, 97 (1998).
- ¹⁹M. Kiwi, J. Mejía-López, R. D. Portugal, and R. Ramírez, *Solid State Commun.* **116**, 315 (2000).
- ²⁰D. S. Deng, X. F. Jin, and R. B. Tao, *Phys. Rev. B* **65**, 172402 (2002).
- ²¹C. Leighton, J. Nogués, H. Suhl, and I. K. Schuller, *Phys. Rev. B* **60**, 12 837 (1999).
- ²²A. P. Malozemoff, *J. Appl. Phys.* **63**, 3874 (1988).
- ²³S. M. Zhou, K. Liu, and C. L. Chien, *Phys. Rev. B* **58**, R14 717 (1998).
- ²⁴N. J. Gökemeijer, J. W. Cai, and C. L. Chien, *Phys. Rev. B* **60**, 3033 (1999).